Available online at www.sciencedirect.com
SCIENCE DIRECT
Protein Expression and Purification 47 (2006) 329–339
Protein Expression & Purification
www.elsevier.com/locate/yprep

Cloning, expression, purification, and properties of a putative plasma membrane hexokinase from *Solanum chacoense* ☆

Éric Claeyssen, Owen Wally, Daniel P. Matton, David Morse, Jean Rivoal *

Institut de Recherche en Biologie Végétale, Université de Montréal, 4101 Rue Sherbrooke est, Montréal, Que., Canada H1X 2B2

Received 13 September 2005, and in revised form 4 November 2005
Available online 5 December 2005

Abstract

A full-length hexokinase cDNA was cloned from *Solanum chacoense*, a wild relative of the cultivated potato. Analysis of the predicted primary sequence suggested that the protein product, ScHK2, may be targeted to the secretory pathway and inserted in the plant plasma membrane, facing the cytosol. ScHK2 was expressed as a hexahistidine-tagged protein in *Escherichia coli*. Expression conditions for this construct were optimized using a specific anti-hexokinase polyclonal anti-serum raised against a truncated version of ScHK2. The full-length recombinant protein was purified to electrophoretic homogeneity using immobilized metal ion affinity chromatography followed by anion exchange chromatography on Fractogel EMD DEAE-650 (S). The purified enzyme had a specific activity of 5.3 μmol/min/mg protein. Its apparent K_ms for glucose (23 μM), mannose (30 μM), fructose (5.2 mM), and ATP (61 μM) were in good agreement with values found in the literature for other plant hexokinases. Hexahistidine-tagged ScHK2 was highly sensitive to pH variations between 7.7 and 8.7. It was inhibited by ADP and insensitive to glucose-6-phosphate. These findings constitute the first kinetic characterization of a homogeneous plant hexokinase preparation. The relevance of ScHK2 kinetic properties is discussed in relation to the regulation of hexose metabolism in plants.

Keywords: Hexokinase; Kinetic analysis; *Solanum chacoense*; Affinity chromatography; *Escherichia coli*; Hexose metabolism; Hexose phosphates

Hexokinase (HK[1], EC 2.7.1.1) is distributed in all kingdoms and catalyzes the irreversible, ATP-dependent phosphorylation of several hexoses including glucose, fructose, mannose, and galactose. HK is thus distinct from glucokinase (GK, EC 2.7.1.2) and fructokinase (FK, EC 2.7.1.4) that are highly specific to glucose and fructose, respectively [1]. In plants, glycolysis begins with sucrose degradation either into glucose and fructose by invertase (EC 3.2.1.26), or into UDP–glucose and fructose by sucrose synthase (EC 2.4.1.13) [2]. Therefore, HK, GK, and FK reactions may constitute a potentially important site for regulation of carbon metabolism as they commit hexoses to cell metabolism [3–6].

Plants typically contain an array of several HK isoforms that differ in their chromatographic and kinetic properties [3,4]. Estimated molecular masses range from 38 to 68 kDa [3,7–9]. Among species studied, the K_m for glucose is low and may vary between 15 and 150 μM. In contrast, the K_m for fructose is always in the millimolar range [4,7,10–15]. The affinity for ATP (K_m between 50 and 560 μM) [4,11,13,15,16] is significantly higher than those of other nucleoside triphosphates [4] or comparable to that of UTP [17], depending on the isoform considered. In maize roots and potato tubers, only some HK isoforms are inhibited by physiological concentrations of glucose-6-phosphate (G6P) (K_i of 0.03–4 mM) or ADP (K_i of 20–110 μM) [4,11,18]. In

☆ This work was supported by a Discovery Grant from the National Science and Engineering Research Council of Canada to J.R.
* Corresponding author. Fax: +1 514 872 9406.
E-mail address: jean.rivoal@umontreal.ca (J. Rivoal).

[1] *Abbreviations used:* HK, hexokinase; GK, glucokinase, FK, fructokinase; G6P, glucose-6-phosphate; Ni–NTA, Ni^{2+}–nitrilotriacetic acid; LB, Luria–Bertani; IPTG, isopropyl β-D-thiogalactoside; IgG, immunoglobulin G; U, unit; T6P, trehalose-6-phosphate; F1P, fructose-1-phosphate; F6P, fructose-6-phosphate; F1,6BP, fructose-1,6-bisphosphate; G1P, glucose-1-phosphate; SDS–PAGE, sodium dodecyl sulfate–polyacrylamide gel electrophoresis.

1046-5928/$ - see front matter © 2005 Elsevier Inc. All rights reserved.
doi:10.1016/j.pep.2005.11.003

addition, regulation by G6P may be pH-dependent [4]. HK isoforms may also vary in their subcellular localizations. Active HK isozymes have been reported in the cytosol [11], in the Golgi complex [16], in the nucleus [19], in the chloroplast stroma [20], on the cytosolic side of the chloroplastic outer membrane [21], and of the mitochondrial outer membrane [22].

In addition to its metabolic role in glycolysis, HK is now broadly accepted as a sugar sensor in eukaryotic cells [19,23–25]. In plants, sugars act as signaling molecules in the control of growth and development during the entire life cycle [26] and regulate expression of genes involved for example in photosynthesis [27,28]. Studies using sugar analogs, metabolic intermediates and transgenic plants, provided evidence that HK is involved in sugar sensing [27,29]. It has also been shown that sugar sensing by HK in plants was not dependent on HK catalytic activity per se, thereby demonstrating that HK has separate functions in glucose metabolism and sensing [30].

The question has often been raised as to how the different HK isoforms of a plant cell contribute to hexose metabolism or sensing [4,5,15,16,20,21,24,31]. Although several plant HKs have been structurally and kinetically characterized [3,4,12–15,21], none of these studies provide evidence that the preparations used for enzyme analyses were electrophoretically pure. As part of our ongoing efforts to better understand the control of hexose metabolism in plants, we describe here the cloning of a HK cDNA from *Solanum chacoense*, a wild relative of the cultivated potato. The corresponding recombinant protein was expressed and purified to electrophoretic homogeneity from *Escherichia coli*. To our knowledge, this is the first kinetic characterization of a pure recombinant plant HK.

Materials and methods

Materials and chemicals

All buffers, chemicals, reagents, and commercial enzymes were of analytical grade and purchased from Sigma Chemical (St. Louis, MO) or Fisher Scientific (Nepean, ON, Canada), unless otherwise stated. PD10 columns used for desalting protein extracts were from G.E. Healthcare (Baie d'Urfé, QC, Canada). Ni^{2+}–nitrilotriacetic acid (Ni–NTA) agarose was from Invitrogen Canada (Burlington, ON, Canada). Platinum *Pfx* used for PCR and the vector pProEx HT, which contains a (6× His) tag and a Tobacco Etch Virus (TEV) protease cleavage site, were from Invitrogen Canada. Restriction enzymes were from MBI Fermentas (Burlington, ON, Canada), and Invitrogen Canada. Primers for PCR and sequencing were from Sigma Genosys (The Woodlands, TX). Fractogel EMD DEAE-650 (S) was from VWR (Mississauga, ON, Canada).

cDNA cloning and sequencing

A *S. chacoense* EST collection was generated in the pBK-CMV vector (Stratagene, La Jolla, CA) from weakly-expressed mRNAs in pistil tissues [32]. A search for a full-length HK in this EST collection led to the identification of a 1.8 kb cDNA encoding a sequence with significant homology to potato HK2 (UniProt Accession No. Q9SQ76). The cDNA (ScHK2) was completely sequenced on both strands using the Big Dye Terminator 2.0 sequencing Kit (Perkin-Elmer, Montreal, QC, Canada) and an ABI 377 automated sequencer.

Generation of full-length ScHK2 and truncated ScHK2 constructs for heterologous expression in E. coli

To express the full-length construct, ScHK2 cDNA in the pBK-CMV vector was first amplified by PCR with Platinum *Pfx* DNA polymerase using the following primers: forward, 5′-ATGAAGAAGGCGACGGTG-3′; reverse, T7 primer. The resulting fragment was digested with *Kpn*I and cloned into *Ehe*I/*Kpn*I-digested pProEX HTb. To express the truncated construct, designated ΔScHK2, the ScHK2 cDNA in pBK-CMV was partially digested with *Eco*RI after complete digestion with *Xho*I, and a 1618-bp restriction fragment encompassing the C-terminal part of ScHK2 was isolated. This fragment was cloned into *Eco*RI/*Xho*I-digested pProEX HTa. The ligated plasmids were used to transform competent *E. coli* (DH5α strain). Restriction digestions confirmed the presence and correct orientation of the inserts. The full-length construct in the expression plasmid carried the entire coding sequence of ScHK2 in frame with a N-terminal 24-amino acid extension containing the (6× His) tag from the expression vector. The deduced amino acid sequence of the resulting fusion protein was 520 amino acids long and had a predicted molecular mass of 56,776 Da. For the truncated ScHK2 (ΔScHK2) construct, the expression plasmid carried the coding sequence of the C-terminal part of ScHK2, in frame with a 29-amino acid extension at the N-terminus. This extension contained the (6× His) tag of the expression vector. The deduced amino acid sequence of the resulting (6× His)ΔScHK2 protein was 482 amino acids long with a predicted mass of 52,817 Da.

Expression and purification of recombinant proteins

For the full-length recombinant ScHK2, *E. coli* carrying the expression plasmid was grown in Fernbach flasks at 37 °C in Luria–Bertani (LB) broth medium (0.5 L volume) to an A_{600} of 0.5–0.7. At this point, isopropyl-β-D-thiogalactoside (IPTG) was added to the culture at a final concentration of 0.6 mM. Unless otherwise mentioned, cultures were left to grow for 1 h at 23 °C. Cells were harvested by centrifugation (15 min at 10,000*g*), and pellets were frozen at −80 °C until used. Purification steps were carried out at 4 °C in native conditions. Bacterial pellets were thawed in 10 mL lysis buffer (50 mM NaH_2PO_4, 10 mM imidazole, 0.3 M NaCl, and 14 mM β-mercaptoethanol) adjusted to pH 8.0 with NaOH, and supplemented with 0.5 mM phenylmethylsulfonylfluoride (PMSF), 0.5 mM benzamidine, 0.5 mM ε-amino-*N*-

caproic acid (ε-CA), 5 μg/mL leupeptin and 0.05% (w/v) Triton X-100. Bacterial cells were lysed using a French pressure cell (18,000 psi). After a 15-min centrifugation at 10,000*g*, the supernatant was desalted on PD10 column pre-equilibrated with lysis buffer. The desalted extract was adsorbed in batch on 1 mL settled volume of Ni–NTA resin pre-equilibrated with lysis buffer during ~75 min. The suspension was then poured into a disposable column (0.5 cm diameter). The column was washed with 16 mL lysis buffer, followed by 12 mL wash buffer (50 mM NaH_2PO_4, 20 mM imidazole, 0.3 M NaCl, and 14 mM β-mercaptoethanol). The bound protein was eluted from the column with 2.5 mL elution buffer (50 mM NaH_2PO_4, 250 mM imidazole, 0.3 M NaCl, and 14 mM β-mercaptoethanol) and collected in five fractions of 0.5 mL. Fractions containing (6× His)ScHK2 were pooled and desalted on PD10 column pre-equilibrated with buffer A (20 mM Tris–HCl, pH 8.2, 5 mM $MgCl_2$, 1 mM DTT, and 10% [v/v] glycerol), and stored overnight at 4 °C. At this stage, the recombinant enzyme preparation contained several contaminating proteins, so an additional purification step was performed. Pooled, desalted fractions were loaded at 0.5 mL/min onto a Fractogel EMD DEAE-650 (S) column (1 × 8 cm) pre-equilibrated in buffer A. The column was connected to a Pharmacia FPLC system and washed with 18 mL buffer A. (6× His) ScHK2 was eluted with a 72-mL linear gradient of 0–500 mM KCl in buffer A, followed by a step gradient to 1 M KCl in buffer A. One milliliter fractions were collected and assayed. ScHK2 activity eluted as one peak between 300 and 425 mM KCl. Aliquots of fractions with HK activity were further analyzed by SDS–PAGE and silver staining [33] as well as immunodetection (see below). Fractions that displayed HK activity and a single band on silver-stained SDS–PAGE gel were concentrated over a Centricon YM30 filter (Millipore, Nepean, ON, Canada). Because small amounts of protein were recovered, protein amounts in concentrated solution were determined by spectrophotometry at 205 nm [34] on a Cary 100 spectrophotometer (Varian Canada, St. Laurent, QC, Canada). Glycerol was added to the concentrated ScHK2 solution at a final concentration of 50% (v/v) and the solution was stored at −20 °C for up to 3 days without any loss of activity. For the partially purified fractions, protein concentration was determined according to Bradford [35], using the Bio-Rad protein assay reagent (Bio-Rad Laboratories, Mississauga, ON, Canada) and bovine serum albumin as standard.

For (6× His)ΔScHK2 protein, *E. coli* (DH5α strain) carrying the expression plasmid was grown at 37 °C in 250 mL LB broth medium and induced with IPTG for 5 h at the same temperature. Cells were harvested by centrifugation (10 min at 10,000*g*), and pellets were frozen at −80 °C until used. Purification steps were carried out at 4 °C. Cell pellets were thawed in 10 mL lysis buffer containing 50 mM Tris–HCl, pH 8.5, 5 mM DTT, 1 mM PMSF, 1 mM benzamidine, 1 mM ε-CA, and 0.1% (w/v) Triton X-100 and disrupted using a French pressure cell (18,000 psi). The extract was centrifuged at 10,000*g* for 25 min. The pellet contained insoluble (6× His)ΔScHK2 and was resuspended in 10 mL buffer B (6 M urea, 0.1 M NaH_2PO_4, and 10 mM Tris–HCl, pH 8.0). After centrifugation at 10,000*g* for 15 min, the clarified sample was adsorbed batchwise with 1 mL Ni–NTA resin equilibrated in buffer B for 1 h. The suspension was then poured in a column (0.5 cm diameter). The column was washed with 4 mL buffer B, followed by 2 mL buffer B adjusted to pH 6.3. The bound protein was eluted from the column with 2 mL buffer B adjusted to pH 5.9, then 2 mL buffer B adjusted to pH 4.5. During elution, 0.5 mL fractions were collected. ΔScHK2 eluted mainly at pH 4.5, as visualized by SDS–PAGE analysis followed by Coomassie blue staining. Fractions containing ΔScHK2 were pooled and adjusted to pH 7.5 with a solution of 1 M Tris–HCl, pH 8.5, and stored frozen until used.

Production and affinity purification of anti-ΔScHK2 immune serum

Purified (6× His)ΔScHK2 was dialyzed for 16 h against 50 mM Tris–HCl, pH 8.5, and 5 mM DTT. The 3-mL solution of dialyzed protein was clarified by centrifugation at 13,000*g* for 25 min. The protein was digested with 200 U of recombinant TEV protease (Invitrogen Canada) for 3 h at 30 °C. The digested protein was separated from the tag and the protease by chromatography on Ni–NTA resin according to the manufacturer's indications. Approximately 200 μg de-tagged recombinant ΔScHK2 was produced using this procedure and subjected to further purification using preparative SDS–PAGE and electroelution as described [36]. Antibodies were raised using a 2-kg New Zealand White rabbit. After collection of the pre-immune serum, de-tagged recombinant ΔScHK2 (120 μg, emulsified in complete Freund's adjuvant) was injected subcutaneously into the back of the rabbit. Booster injections were given at days 14 and 21 with 40 μg of recombinant ΔScHK2 emulsified in incomplete Freund's adjuvant. Final bleed was performed on day 42 by cardiac puncture. The serum was collected after centrifugation at 1500*g*, frozen in aliquots in liquid N_2, and kept at −80 °C. Crude anti-serum was purified by affinity against 15 μg recombinant ΔScHK2 using a method modified from [37]. Briefly, the membrane strip corresponding to (6× His)ΔScHK2 was identified by staining with Ponceau S and cut out from the blot. This strip was incubated for 1 h in 1.5 mL blocking buffer containing Tris-buffered saline Tween 20 (TBST) buffer (0.5 M Tris–HCl, pH 7.6, 1.5 M NaCl, 0.5% (v/v) Tween 20, and 0.2% (w/v) NaN_3) supplemented with 3% (w/v) powdered milk. The blot was then washed 3 times for 1 min with 1.5 mL TBST buffer and incubated for 1 h with 1.2 mL crude anti-serum. After removal of anti-serum, the strip was washed 4 times for 1 min with 1.5 mL TBST buffer, then incubated for 2 min with 1.5 mL of elution buffer (20 mM glycine–HCl, pH 3.0, 0.5 M NaCl, 0.25% [v/v] Tween 20, and 0.04% [w/v] NaN_3). Eluted IgGs were collected, neutralized with a solution of 1 M Tris–HCl, pH 8.5, and adjusted to 0.5% (w/v) BSA. Purified IgGs were frozen in liquid N_2 and stored at −80 °C until used.

SDS–PAGE and immunoblot analysis of ScHK2

SDS–PAGE analyses on 12% acrylamide gels and electrotransfer to polyvinylidene difluoride (PVDF) membranes were performed as described previously [38,39]. For immunodetection, blots were incubated with affinity-purified anti-ΔScHK2 IgGs (1/15 dilution). Polypeptides were detected using an anti-rabbit alkaline phosphatase-tagged secondary antibody (1/10,000 dilution) (Promega, Nepean, ON, Canada). The phosphatase reaction was visualized with 5-bromo-4-chloro-3-indoyl phosphate (BCIP) and nitroblue tetrazolium (NBT), and allowed to develop for 4 to 30 min at 30 °C. Immunoblots incubated with the pre-immune serum gave negative results (data not shown).

Hexokinase activity assay

HK activity assays were conducted according to a protocol modified from [5]. The HK reaction was coupled to the glucose-6-phosphate dehydrogenase (EC 1.1.1.49) reaction, and assayed at 30 °C by monitoring NAD^+ reduction at 340 nm using a VersaMax (Molecular Devices, Sunnyvale, CA, USA) microplate reader. The 200-μL reaction mixture contained 50 mM Tris–HCl, pH 8.0, 50 mM KCl, 5 mM $MgCl_2$, 5 mM DTT, 0.3 mM NAD^+, 1 mM ATP, 1.4 U/mL glucose-6-phosphate dehydrogenase from *Leuconostoc mesenteroides* and (i) 5 mM glucose for glucokinase (EC 2.7.1.2) activity, (ii) 6.7 U/mL phosphoglucose isomerase (EC 5.3.1.9) and 5 mM fructose for fructokinase (EC 2.7.1.4) activity, or (iii) 3.5 U/mL phosphoglucose isomerase, 3.5 U/mL phosphomannose isomerase (EC 5.3.1.8), and 5 mM mannose for mannokinase (EC 2.7.1.7) activity. Reaction rates were linear with time and proportional to the amount of enzyme added to the assay within a range spanning one order of magnitude (data not shown). To determine HK activity towards 3-*O*-methylglucose and to study HK inhibition by glucose-6-phosphate, a coupled-enzyme assay with pyruvate kinase (EC 2.7.1.40) and lactate dehydrogenase (EC 1.1.1.28) was used. The conditions to measure initial rates of ADP production in this assay were adapted from [5]. The assay mixture (200 μL) contained 50 mM Tris–HCl, pH 8.0, 50 mM KCl, 5 mM $MgCl_2$, 5 mM DTT, 0.15 mM NADH, 1 mM ATP, 0.5 mM phosphoenolpyruvate, 1 mM glucose (or 100 mM 3-*O*-methylglucose), 3.1 U/mL pyruvate kinase, and 15.4 U/mL lactate dehydrogenase. Assays were initiated by addition of enzyme preparation and corrected for background activity by omitting substrate from the reaction mixture. One unit (U) of HK activity is defined as the amount of enzyme that catalyzes the production of 1 μmol of G6P or ADP per minute at 30 °C.

Characterization of ScHK2 kinetic properties

For all analyses, presented data are means ± SE of determinations carried out on three independent enzyme preparations with quadruplicate assays unless otherwise mentioned. The effect of pH on ScHK2 activity was studied using a three-component buffer to maintain a constant ionic strength throughout the pH range [40]. The Tris–HCl buffer used in the standard reaction mixture described above was therefore replaced with 0.05 M acetic acid, 0.05 M 2-(*N*-morpholino)-ethanesulfonic acid (MES) and 0.1 M Tris–HCl adjusted at different pH values with 1 M NaOH or HCl. The assay pH was measured directly in the reaction mixture using a microelectrode immediately after completion of the spectrophotometric assay. Apparent K_m (K_{mapp}) values were calculated from the Michaelis–Menten equation using a non-linear least-squares regression program (SigmaPlot 8.0, SPSS, Chicago, IL, USA). k_{cat} values were calculated from the V_{max} of Michaelis–Menten plots and using a subunit molecular mass of 56,776 Da.

Results and discussion

Characteristics of the protein sequence encoded by ScHK2 and implications for the production of a recombinant ScHK2 carrying a (6× His) epitope tag at the N-terminus

A full-length cDNA encoding ScHK2 was isolated from *S. chacoense* (GenBank Accession No. DQ177440). The cDNA was 1793 nt long and contained a 496 amino acid ORF. Deduced amino acid sequence from the ORF predicted a 53,751 Da polypeptide with an isoelectric point of 6.07. Analysis of the polypeptide sequence (Fig. 1) showed a high degree of amino acid sequence similarity (>97%) with *Nicotiana sylvestris* HK3, *Solanum tuberosum* HK2, and *Solanum esculentum* HK2, which are all members of the *Solanaceae* family.

The existence of stromal and membrane-bound HKs in plants [20,21] as well as the fact that there was a stretch of hydrophobic amino acids at the N-terminus of the protein (Fig. 1) prompted us to investigate the predicted subcellular localization of ScHK2 (Table 1). The sequence was analyzed with TargetP 1.1 [41] available at http://www.cbs.dtu.dk/services/TargetP/, Protein Prowler 1.1 [42] available at http://pprowler.imb.uq.edu.au and PSORT [43] available at http://psort.ims.u-tokyo.ac.jp/ (Table 1). Targeting of ScHK2 to the secretory pathway and endoplasmic reticulum membrane obtained the highest scores in these analyses. Targeting to other cell compartments including the mitochondrion or the chloroplast, appeared much less plausible (Table 1). The SignalP 3.0 program [44,45] available at http://www.cbs.dtu.dk/services/SignalP/ predicted a signal peptide at the N-terminus, and a possible cleavage site between amino acid residues 20 and 21. Signal peptides are known to control the entry of eukaryotic and prokaryotic proteins in the secretory pathway. Typical secretory pathway signal peptides contain 1 or more basic residues at the N-terminus, followed by a hydrophobic region of 7 or more amino acids and a neutral polar region that may be recognized by leader peptidases [45,46]. These features are consistent with the 2 basic Lys residues at positions 2 and 3, the hydrophobic region between positions 6 and 17 and the

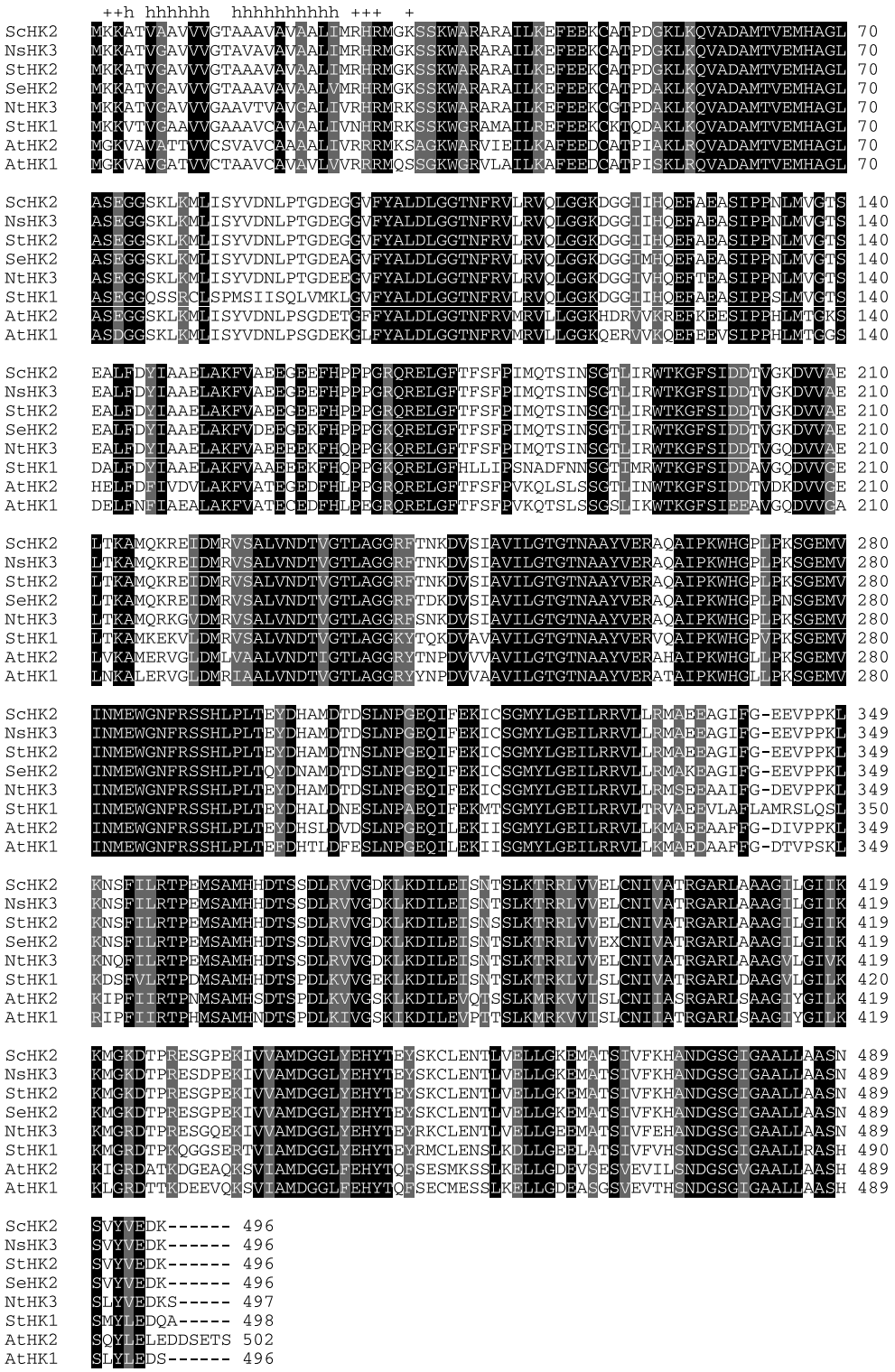

Fig. 1. Multiple amino acid sequence alignment of eight plant HKs. The derived amino acid sequence of the *S. chacoense* HK2 cDNA was compared to those of other plant HKs using CLUSTAL W (1.74). Identical and similar amino acid residues are darkened and shaded, respectively. The distribution of basic (+) and hydrophobic (h) amino acid residues in the N-terminal region of SCHK2 is indicated. Accession numbers of sequences used here are as follows: *S. chacoense* ScHK2 (GenBank DQ177440), *N. sylvestris* NsHK3 (UniProt Q6BDB7), *S. tuberosum* StHK2 (UniProt Q9SQ76), *S. esculentum* SeHK2 (UniProt Q9FR27), *N. tabacum* NtHK3 (UniProt Q6Q8A4), *S. tuberosum* StHK1 (UniProt O64390), *A. thaliana* AtHK2 (UniProt P93834), and *A. thaliana* AtHK1 (UniProt Q42525).

Table 1
Prediction of the subcellular targeting for the ScHK2 protein sequence in plants

Program	Subcellular targeting or localization	Score
TargetP 1.1	cTP	0.15
	mTP	0.13
	SP	**0.68**
	Other	0.02
Protein Prowler 1.1	cTP	0.00
	mTP	0.04
	SP	**0.91**
	Other	0.04
PSORT	**ERM**	**0.82**
	ERL	0.10
	PM	0.19
	EC	0.10

The deduced primary sequence was analyzed using TargetP 1.1, PSORT, and Protein Prowler 1.1. The scores indicate the likelihood of targeting to a particular compartment by the different programs. The predicted subcellular localization for each program appears in boldface. cTP, chloroplastic targeting; mTP, mitochondrial targeting; SP, secretory pathway; ERM, endoplasmic reticulum membrane; ERL, endoplasmic reticulum lumen; PM, plasma membrane; EC, extracellular.

putative signal peptidase site AVA between residues 18 and 20 in the ScHK2 sequence (Fig. 1). However, this topology predicts that ScHK2 is secreted in the plant apoplastic fluid. The secretion of ScHK2 outside of the cell seems improbable since (i) secretion of HK has never been described and (ii) there is no known source of ATP in the plant apoplast. It thus seems more likely that the signal peptide continues on to residue 23. In this case, the hydrophobic region would be followed by a more basic region (MRHRMGK) than that found at the N-terminus (Fig. 1). The remainder of the protein is predominantly hydrophilic (Fig. 2A) and does not present any evidence of another transmembrane domain. According to the 'positive-inside rule' [47], these particular sequence characteristics are consistent with the prediction that in plant cells, ScHK2 would be anchored by its N-terminal domain in the plasma membrane, with the bulk of the protein facing the cytoplasm (Fig. 2B).

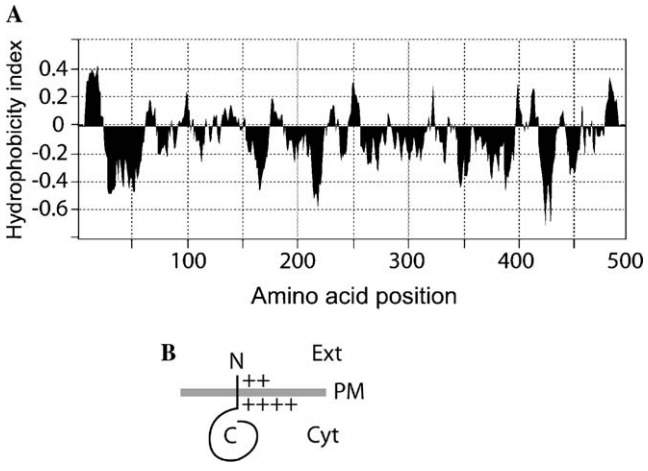

Fig. 2. Hydrophobicity plot and predicted topology of ScHK2. (A) Hydrophobicity index was calculated with Mac vector 7.0 and plotted as a function of amino acid position. (B) Proposed topology of ScHK2 in the plasma membrane. The scheme represents ScHK2 anchored in the plasma membrane (PM). ScHK2 N- and C-termini are respectively localized in the extracellular (Ext) and cytoplasmic (Cyt) compartments. The proposed localization of N-terminal domain basic residues (+) on each side of the membrane is also depicted.

The construction of the full-length recombinant protein added the sequence NH_2-MSYYHHHHHHDYDIPTTE TLYFQG- to the N-terminus of ScHK2. The stretch of His residues places a predominantly positively charged region upstream of the signal peptide and might be expected to have a topology exactly opposite to that of the native protein [47]. Efficient translocation of heterologous proteins is possible in *E. coli* [46] and we would predict that (6× His)ScHK2 could behave as a secretory protein.

Expression and purification of recombinant ScHK2

Our first attempts to express (6× His)ScHK2 in *E. coli* cells were met with limited success (Fig. 3A), in agreement with our prediction that (6× His)ScHK2 secretion could interfere with accumulation of the protein. We thus constructed a truncated form of the protein lacking the first 47 amino acids of ScHK2 (ΔScHK2). This deletion removed the entire predicted signal peptide. The ΔScHK2 construct could be expressed in bacteria to levels detectable by SDS–PAGE analysis (Fig. 3B), however, the protein was insoluble and inactive. We nevertheless took advantage of this high level of expression to raise an anti-serum against ΔScHK2. This immune serum was used to optimize the conditions for production of the full-length (6× His) ScHK2.

Using the anti-ΔScHK2 immune serum, the steady-state levels of (6× His)ScHK2 were monitored in *E. coli* cells and in the culture medium over an induction period of 15–240 min at 23 and 37 °C (Figs. 4A and B). The band present in non-induced bacteria (−IPTG lane), may reflect leakiness in the control of the *trc* promoter over ScHK2 expression. Nonetheless, induction of (6× His)ScHK2 expression was efficient as evidenced by more intense bands in +IPTG

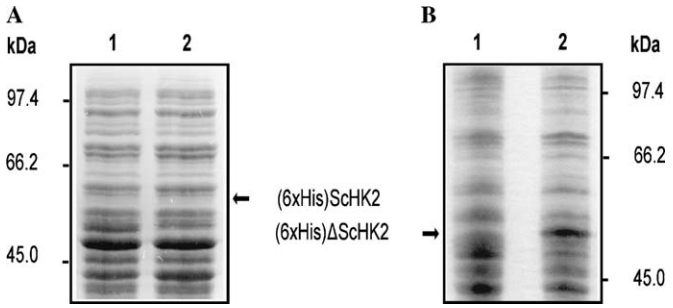

Fig. 3. SDS–PAGE analysis of (6× His)ScHK2 (A) and (6× His)ΔScHK2 (B) expression in *E. coli*. Lane 1: non-induced, total crude extract; lane 2: total crude extract after 4 h induction at 37 °C with IPTG. The running positions of molecular mass standards are indicated on the left, those of ScHK2 and ΔScHK2 are indicated by arrows. Fifty microliters of culture was loaded on each lane.

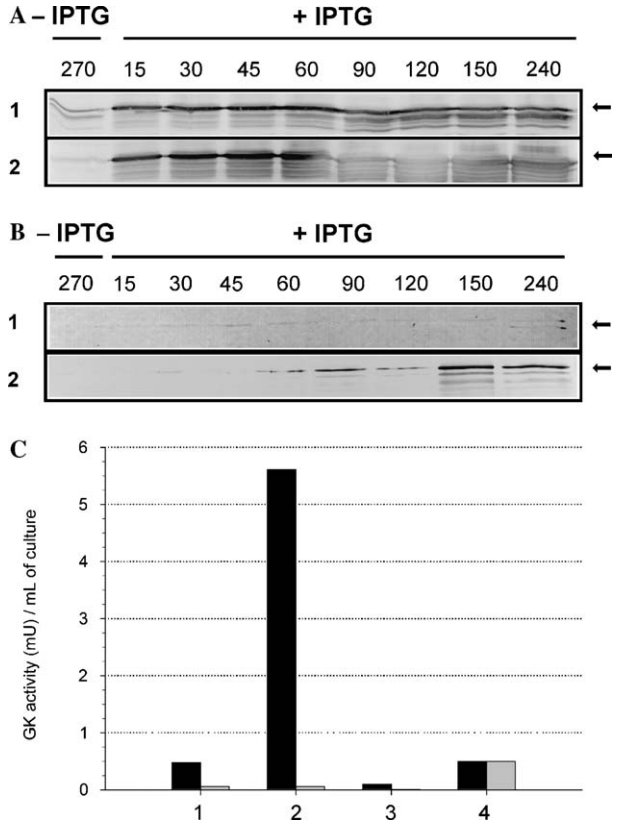

Fig. 4. Immunoblot analysis (A and B), and HK activity assay (C) on *E. coli* cell cultures expressing (6× His)ScHK2. (A) Immunoblot analysis of ScHK2 expressed in *E. coli* cell pellets after induction of the cultures with or without IPTG for 15–270 min at 23 °C (blot 1) or at 37 °C (blot 2). Control (non-induced) cells are analyzed on the (−IPTG) lane. (B) Immunoblot analysis of ScHK2 in culture medium of *E. coli* cell cultures used in (A). The running position of ScHK2 is indicated by an arrow on the various blots. The lanes contain equivalents of 50 μL of culture in (A) and of 18 μL of culture in (B). (C) HK activity was assayed in bacterial cell extracts and in the culture medium concentrated over a Centricon YM3 membrane. Data are representative of at least two separate experiments for cultures incubated with or without IPTG for 240 min. Black bars, induction at 23 °C. Grey bars, induction at 37 °C. 1, −IPTG cells; 2, +IPTG cells; 3, medium of −IPTG cells; 4, medium of +IPTG cells.

lanes than in the −IPTG lane (Fig. 4A). ScHK2 steady-state levels in cells induced for 15–60 min were higher at 37 than at 23 °C (Fig. 4A). However, those levels declined beyond 60 min of induction, with a more dramatic effect at 37 °C. This decline coincided with rising ScHK2 levels in the culture medium, especially at 37 °C (Fig. 4B). We therefore investigated HK activity in bacteria and in their culture medium after 240 min of induction (Fig. 4C). Levels of HK activity were extremely low in bacteria and in the medium when induction of ScHK2 expression was performed at 37 °C. Contrastingly, HK activity was much higher (5.6 mU/mL of culture) in bacteria induced at 23 °C. HK activity was slightly higher in the culture medium than in cells at 37 °C, in accordance with the immunoblot data. However, HK activity levels in the culture medium remained much lower than the levels found in cells at 23 °C. Taken together, these data suggest that ScHK2 was secreted from *E. coli* cells during induction, and that this effect was more pronounced at 37 than at 23 °C. For reasons that we did not investigate further, cell cultures induced at 37 °C displayed less HK activity than those induced at 23 °C. Lastly, secretion of ScHK2 into the culture medium seemed to result in a loss of activity. Based on these results, we decided to purify the ScHK2 protein from *E. coli* cell cultures induced for 60 min at 23 °C. Indeed, these conditions produced active recombinant ScHK2 and produced the strongest immunoblot signal during the induction time course.

Results of a typical purification procedure are presented in Table 2. The (6× His)ScHK2 protein was purified over 260 fold to a specific activity of 5.3 U/mg protein. To our knowledge, this corresponds to the highest specific activity ever reported for a plant hexokinase [4,11,13,14,16,21,48–50]. (6× His)ScHK2 was purified to electrophoretic homogeneity as shown by silver staining of SDS gel (Fig. 5, lane 1). An immunoblot analysis carried out on the purified preparation (Fig. 5, lane 2) showed that purified

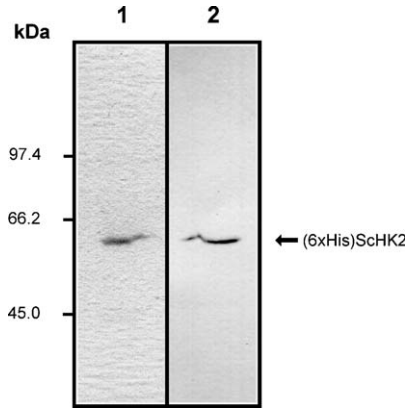

Fig. 5. Analysis of purified (6× His)ScHK2 by SDS–PAGE (1) and immunoblot (2). The gel was silver-stained as described in Materials and methods. Immunoblot was carried using affinity-purified IgGs. The running positions of molecular mass standards are indicated on the left.

Table 2
Purification of recombinant ScHK2 from *E. coli* cells

Step	Total activity (U)[a]	Total protein (mg)	Specific activity (U/mg protein)	Yield (%)	Purification (fold)
Desalted extract	2.3	107.2	0.02	100	1
Ni–NTA	0.5	0.7	0.71	22	35.5
DEAE Fractogel	0.10	0.02	5.29	4	265

[a] Activity unit expressed in μmol/min with glucose as substrate.

(6× His)ScHK2 was free of degradation products. This purified protein was used to conduct kinetic studies.

Effects of pH on ScHK2 activity

ScHK2 displayed an optimum pH at the fairly high pH value of 8.7 (Fig. 6). Moreover, ScHK2 activity decreased sharply (3-fold) within a narrow range from pH 8.7 down to pH 7.7. Such a sharp pH curve resembled that of HK1 in potato tuber [4,13] but contrasted with the broad pH response observed for most plant HKs [48–50]. Therefore, ScHK2 activity may be quite responsive to slight changes in physiological pH.

Kinetic behavior of ScHK2

We determined the kinetic constants of pure (6× His)ScHK2 for various substrates (Table 3). Recombinant ScHK2 protein exhibited comparable affinity for glucose ($K_{mapp} = 23\,\mu M$) and mannose ($K_{mapp} = 30\,\mu M$). The enzyme could phosphorylate both aldoses with a relatively high catalytic efficiency ($k_{cat}/K_{mapp} > 120$ s/mM). In contrast, ScHK2 had lower affinity for fructose ($K_{mapp} =$ 5.2 mM) and a catalytic efficiency that was more than 100 fold lower than with glucose and mannose. Therefore, (6× His)ScHK2 displayed typical kinetic characteristics of a plant HK [4,21,49]. In heterotrophic organs such as potato tuber, cytosolic glucose concentrations can reach 30 mM while concentrations of mannose and fructose are respectively more than three orders of magnitude lower and not detected [51]. Consequently, phosphorylation of glucose in tubers by ScHK2 is most likely not limited by in vivo glucose concentrations. Among nucleoside triphosphates, ATP was the preferred substrate ($K_{mapp} = 61\,\mu M$) with a catalytic efficiency that was at least 10 times higher than with other nucleoside triphosphates (Table 3). Similar results were obtained with HKs purified from potato tuber [4] and from developing maize kernels [50]. Farré et al. [51] reported ATP cytosolic concentrations in excess of 200 μM ATP in potato tuber cells, and developing wheat seeds contain 250 nmol/g FW [52]. ATP is therefore probably not limiting for ScHK2 in plant cells under normal conditions. The K_{mapp} (UTP) was in the millimolar range. Despite the fact that UTP is generally fairly abundant [51,52], the estimate of its cytosolic concentration is still much lower than the K_{mapp}. It is therefore doubtful that UTP plays a significant role in hexose phosphorylation by ScHK2.

We next tested the effect of various compounds on (6× His)ScHK2 activity. The choice of effectors was made either because of their physiological relevance, or because of their use in studies on the role of HK in sugar sensing (Table 4). Amongst them, fructose, sucrose, fructose-1-phosphate (F1P), fructose-6-phosphate (F6P), fructose-1,6-bisphosphate (F1,6BP), and glucose-1-phosphate (G1P) were without any important effect on (6× His)ScHK2 activity. On the contrary, the recombinant protein was strongly inhibited by mannose, most plausibly due to the high affinities of (6× His)ScHK2 for both glucose and mannose (Table 3). 3-*O*-Methylglucose was not an inhibitor. However, it could serve as substrate for (6× His)ScHK2 (data not shown), thus corroborating previous observations by [53]. Trehalose-6-phosphate (T6P) has been proposed to regulate plant glycolysis through inhibition of HK activity [54,55], by analogy to the yeast model [56]. However, we did not observe any inhibition by T6P (Table 4), similarly to previous observations with other plant HKs [21,57,58]. Glucosamine, a specific inhibitor of HK [59], has been used in studies investigating the implication of HK in sugar sensing [16,27,60]. (6× His)ScHK2 was more sensitive to glucosamine than other plant HKs characterized so far [14,21,60], with 50% inhibition at 5 mM. Interestingly, [16] noted that a membrane-bound HK was more sensitive to glucosamine than a soluble isoform in maize roots. In contrast to mammalian HKs, yeast and most plant enzymes are not subject to feedback regulation by G6P [55]. Nevertheless, some pH-dependent inhibition by G6P has been observed for potato tuber HK1 [4] as well as for tomato fruit GK [5]. In our study, we used up to 10 mM G6P since cytosolic levels of 0.4–12 mM have been measured or

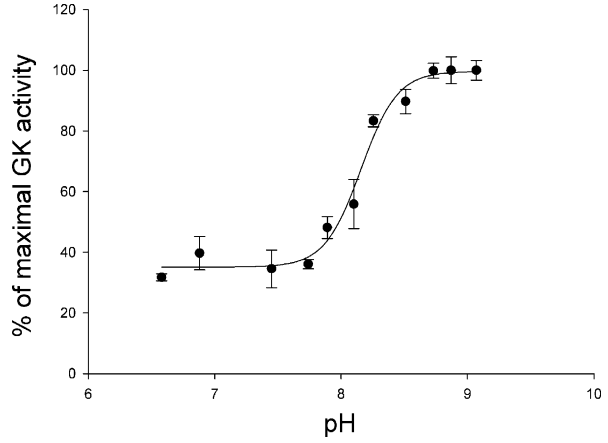

Fig. 6. Effects of pH variation on ScHK2 activity. Values are representative of data from two separate purifications (100% = s3.1 mU using glucose as substrate).

Table 3
Kinetic constants of pure ScHK2 [a]

Substrate	K_{mapp} (mM)	k_{cat} (s^{-1})	k_{cat}/K_{mapp} ($mM^{-1}s^{-1}$)
D-Glucose	0.023 ± 0.003	5.01 ± 0.75	218
D-Fructose	5.2 ± 0.4	3.78 ± 1.13	0.7
D-Mannose	0.030 ± 0.004	3.69 ± 0.47	123
ATP	0.061 ± 0.01	3.50 ± 0.37	57
TTP	0.231	1.42	6.1
GTP	0.231	0.85	3.7
UTP	2.2	3.02	1.4
CTP	2.0	1.61	0.8

[a] For hexoses and ATP, kinetic parameters are given as means ± SE of values from three independent enzyme preparations. Values for TTP, GTP, UTP, and CTP, are representative of two independent enzyme preparations.

Table 4
Effect of various metabolites on (6× His)ScHK2 activity[a]

Effector added	Effector concentration (mM)	% Activity mean ± SE
None	—	100 ± 3
Fructose	1	92 ± 1.4
	10	94 ± 1.2
Mannose	1	46 ± 1.4
	10	12 ± 1.5
Sucrose	1	91 ± 0.4
	10	91 ± 2.2
Fructose-1-phosphate	0.1	90 ± 0.2
	0.25	86 ± 1.5
	0.5	93 ± 4.9
	1	101 ± 0.2
Fructose-6-phosphate	1	96 ± 1.2
	5	98 ± 1.9
	10	100 ± 0.5
Fructose-1,6-bisphosphate	1	88 ± 4.7
	10	101 ± 3.1
Glucose-1-phosphate	1	95 ± 1.4
	10	104 ± 1.5
Glucose-6-phosphate	0	101 ± 0.6
	0.05	92 ± 0.1
	0.1	93 ± 3.1
	0.5	97 ± 3.8
	1	97 ± 1.7
	5	116 ± 4.5
	10	128 ± 5.5
Trehalose-6-phosphate	0.2	93 ± 0.6
	0.5	92 ± 0.6
	1	94 ± 1
3-*O*-Methylglucose	1	91 ± 0.7
	10	89 ± 1.3
	100	92 ± 1.6
Glucosamine	0.5	90 ± 2.4
	1	82 ± 6.0
	5	54 ± 3.8
	20	33 ± 2.4
	50	20 ± 2.0
	100	13 ± 2.5
ADP	0.05	57 ± 1.3
	0.1	41 ± 0.9
	0.5	17 ± 0.9
	1	13 ± 0.8
	2.5	11 ± 0.5

[a] Listed metabolites were analyzed in the standard assay medium with a saturating concentration of glucose. The effect is reported as a percentage of the control (100% = 30 mU). Activities are given as means ± SE of values from three independent enzyme preparations. For analyzing the effect of glucose-6-phosphate, a different coupled enzyme assay using PK and LDH was utilized. The 0 mM control for this assay is included in the table.

assumed for different plant tissues [4,51,61]. G6P did not inhibit ScHK2 at pH 8.0 (Table 4), in agreement with data on some other plant HKs [4,11,49,50]. There was even a slight activity increase at high G6P concentrations. Similar results were obtained at pH 7.0 (data not shown). Lastly, we observed a strong inhibitory effect of ADP since 0.05–2.5 mM ADP inhibited ScHK2 activity by 40–90% (Table 4). Strong inhibition by ADP has been reported elsewhere [11,14,16,18]. This finding may suggest a major role for the ATP/ADP ratio in regulating ScHK2 activity in plants [16].

Conclusions

Despite its cardinal importance in plant carbohydrate metabolism and sugar sensing, a hexokinase of plant origin had never been previously purified to homogeneity. We circumvented the initial difficulties in the production of (6× His)ScHK2 by expression of a truncated form of the protein in *E. coli*. Removal of the first 47 amino acids in the construct resulted in high levels of expression for (6× His) Δ ScHK2 that permitted the generation of an anti-HK immune serum. By using affinity-purified anti-HK IgGs and HK activity assays we were able to address the reasons causing low levels of (6× His)ScHK2 expression. We found that (6× His)ScHK2 was produced and secreted into the culture medium at 37 °C, although the protein was inactive at that temperature. When expressed at 23 °C, (6× His)ScHK2 was active and accumulated in modest but detectable levels in cells during the first hour of induction. These conditions were chosen to produce an electrophoretically homogeneous recombinant plant HK preparation for characterization.

Analysis of the ScHK2 sequence predicted that the protein be membrane-anchored by its N-terminal hydrophobic region. In the absence of any additional targeting cues, the most likely destination of ScHK2 is the plasma membrane. Wiese et al. [21] described the first membrane-localized plant HK. This isoform was inserted into the chloroplast outer envelope, facing the cytosolic side in spinach leaf cells. The authors suggested that the protein could be involved in the energization of glucose exported from plastids into the cytosol. By analogy, we propose that ScHK2 constitutes a major control step in hexose import into sink cells, a role that would reflect its predicted subcellular localization and topology. It is worth noting that the features discovered in the N-terminal region of ScHK2 are also present on other plant HKs (see Fig. 1). By phosphorylating fructose and particularly glucose produced from sucrose degradation, ScHK2 may help maintain a concentration gradient of these hexoses across the plasma membrane, thereby facilitating their import into the cytosol [62]. Such import would rely on adequate energy charge as ScHK2 may be highly sensitive to rising cytosolic ADP levels (Table 4). This would ensure that feeding of cytosolic glycolysis with hexoses is coupled to ATP generation by mitochondrial oxidative phosphorylation. We further hypothesize that hypoxic conditions, may be detrimental to the function of ScHK2. Indeed, under oxygen deprivation, cytosolic ADP levels increase 2–3-fold to 200 μM [63], while cytosolic pH drops from pH 7.5 to 6.5 [64]. In anoxic maize root tips, Bouny and Saglio [65] have identified hexose phosphorylation as a major controlling step in hexose catabolism. If ScHK2 is present in hypoxic plant tissues, its inhibition by ADP and acidic pH conditions may very well participate to a decrease in hexose phosphorylation. The expression pattern of ScHK2 in plant tissues is still unknown but the estimation of HK protein steady-state levels will be facilitated by the immune serum generated in this study.

References

[1] M.L. Cardenas, A. Cornish-Bowden, T. Ureta, Evolution and regulatory role of the hexokinases, Biochim. Biophys. Acta 1401 (1998) 242–264.

[2] W.C. Plaxton, The organization and regulation of plant glycolysis, Annu. Rev. Plant Physiol. Plant Mol. Biol. 47 (1996) 185–214.

[3] A. Renz, L. Merlo, M. Stitt, Partial purification from potato tubers of three fructokinases and three hexokinases which show differing organ and developmental specificity, Planta 190 (1993) 156–165.

[4] A. Renz, M. Stitt, Substrate specificity and product inhibition of different forms of fructokinases and hexokinases in developing potato tubers, Planta 190 (1993) 166–175.

[5] E. Martinez-Barajas, D.D. Randall, Purification and characterization of a glucokinase from young tomato (*Lycopersicon esculentum* L. Mill.) fruit, Planta 205 (1998) 567–573.

[6] J.V. Pego, S.C. Smeekens, Plant fructokinases: a sweet family get-together, Trends Plant Sci. 5 (2000) 531–536.

[7] T.J. Higgins, J.S. Easterby, Wheatgerm hexokinase: physical and active-site properties, Eur. J. Biochem. 45 (1974) 147–160.

[8] J.A. Miernyk, D.T. Dennis, Mitochondrial, plastid, and cytosolic isozymes of hexokinase from developing endosperm of *Ricinus communis*, Arch. Biochem. Biophys. 226 (1983) 458–468.

[9] Y.T. Yamamoto, R.T.N. Prata, J.D. Williamson, M. Weddington, D.M. Pharr, Formation of a hexokinase complex is associated with changes in energy utilization in celery organs and cells, Physiol. Plantarum 110 (2000) 28–37.

[10] N. Dai, A.A. Schaffer, M. Petreikov, D. Granot, *Arabidopsis thaliana* hexokinase cDNA isolated by complementation of yeast cells, Plant Physiol. 108 (1995) 879–880.

[11] A. Galina, M. Reis, M.C. Albuquerque, A.G. Puyou, M.T. Puyou, L. de Meis, Different properties of the mitochondrial and cytosolic hexokinases in maize roots, Biochem. J. 309 (1995) 105–112.

[12] N. Dai, A. Schaffer, M. Petreikov, Y. Shahak, Y. Giller, K. Ratner, A. Levine, D. Granot, Overexpression of *Arabidopsis* hexokinase in tomato plants inhibits growth, reduces photosynthesis, and induces rapid senescence, Plant Cell 11 (1999) 1253–1266.

[13] J. Veramendi, U. Roessner, A. Renz, L. Willmitzer, R.N. Trethewey, Antisense repression of hexokinase 1 leads to an overaccumulation of starch in leaves of transgenic potato plants but not to significant changes in tuber carbohydrate metabolism, Plant Physiol. 121 (1999) 123–134.

[14] T. Menu, C. Rothan, N. Dai, M. Petreikov, C. Etienne, A. Destrac-Irvine, A. Schaffer, D. Granot, B. Ricard, Cloning and characterization of a cDNA encoding hexokinase from tomato, Plant Sci. 160 (2001) 209–218.

[15] J.O. Giese, K. Herbers, M. Hoffmann, R.B. Klosgen, U. Sonnewald, Isolation and functional characterization of a novel plastidic hexokinase from *Nicotiana tabacum*, FEBS Lett. 579 (2005) 827–831.

[16] W.S. da Silva, G.L. Rezende, A. Galina, Subcellular distribution and kinetic properties of cytosolic and non-cytosolic hexokinases in maize seedling roots: implications for hexose phosphorylation, J. Exp. Bot. 52 (2001) 1191–1201.

[17] C. Schnarrenberger, Characterization and compartmentation, in green leaves, of hexokinases with different specificities for glucose, fructose, and mannose and for nucleoside triphosphates, Planta 181 (1990) 249–255.

[18] A. Galina, L. Logullo, E.F. de Sousa, G.L. Rezende, W.S. da Silva, Sugar phosphorylation modulates ADP inhibition of maize mitochondrial hexokinase, Physiol. Plant. 105 (1999) 17–23.

[19] J. Sheen, L. Zhou, J.C. Jang, Sugars as signaling molecules, Curr. Opin. Plant Biol. 2 (1999) 410–418.

[20] T. Olsson, M. Thelander, H. Ronne, A novel type of chloroplast stromal hexokinase is the major glucose-phosphorylating enzyme in the moss *Physcomitrella patens*, J. Biol. Chem. 278 (2003) 44439–44447.

[21] A. Wiese, F. Groner, U. Sonnewald, H. Deppner, J. Lerchl, U. Hebbeker, U. Flugge, A. Weber, Spinach hexokinase I is located in the outer envelope membrane of plastids, FEBS Lett. 461 (1999) 13–18.

[22] P. Giegé, J.L. Heazlewood, U. Ressner-Tunali, H. Millar, A.R. Fernie, C.J. Leaver, L.J. Sweetlove, Enzymes of glycolysis are functionally associated with the mitochondrion in *Arabidopsis* cells, Plant Cell 15 (2003) 2140–2151.

[23] F. Rolland, J. Winderickx, J.M. Thevelein, Glucose-sensing mechanisms in eukaryotic cells, Trends Biochem. Sci. 26 (2001) 310–317.

[24] G.N. Harrington, D.R. Bush, The bifunctional role of hexokinase in metabolism and glucose signaling, Plant Cell 15 (2003) 2493–2496.

[25] W.B. Frommer, W.X. Schulze, S. Lalonde, Hexokinase, jack-of-all-trades, Science 300 (2003) 261–263.

[26] F. Rolland, B. Moore, J. Sheen, Sugar sensing and signaling in plants, Plant Cell 14 (2002) S185–S205.

[27] J.C. Jang, J. Sheen, Sugar sensing in higher plants, Plant Cell 6 (1994) 1665–1679.

[28] K.E. Koch, Carbohydrate-molulated gene expression in plants, Annu. Rev. Plant Physiol. Plant Mol. Biol. 47 (1996) 509–540.

[29] J.C. Jang, P. Leon, L. Zhou, J. Sheen, Hexokinase as a sugar sensor in higher plants, Plant Cell 9 (1997) 5–19.

[30] B. Moore, L. Zhou, F. Rolland, Q. Hall, W.H. Cheng, Y.X. Liu, I. Hwang, T. Jones, J. Sheen, Role of the *Arabidopsis* glucose sensor HXK1 in nutrient, light, and hormonal signaling, Science 300 (2003) 332–336.

[31] T.C. Fox, B.J. Green, R.A. Kennedy, M.E. Rumpho, Changes in hexokinase activity in *Echinochloa phyllopogon* and *Echinochloa crus-pavonis* in response to abiotic stress, Plant Physiol. 118 (1998) 1403–1409.

[32] S. Lantin, M. O'Brien, D.P. Matton, Pollination, wounding and jasmonate treatments induce the expression of a developmentally regulated pistil dioxygenase at a distance, in the ovary, in the wild potato *Solanum chacoense* Bitt., Plant Mol. Biol. 41 (1999) 371–386.

[33] W. Wray, T. Boulikas, V.P. Wray, R. Hancock, Silver staining of proteins in polyacrylamide gels, Anal. Biochem. 118 (1981) 197–203.

[34] C.M. Stoscheck, Quantitation of protein, Methods Enzymol. 182 (1990) 50–68.

[35] M.M. Bradford, A rapid and sensitive method for the quantitation of microgram quantities of protein utilizing the principle of protein–dye binding, Anal. Biochem. 72 (1976) 248–254.

[36] S. Dorion, Parveen, J. Jeukens, D.P. Matton, J. Rivoal, Cloning and characterization of a cytosolic isoform of triosephosphate isomerase developmentally regulated in potato leaves, Plant Sci. 168 (2005) 183–194.

[37] W.C. Plaxton, Molecular and immunological characterization of plastid and cytosolic pyruvate kinase isozymes from castor-oil-plant endosperm and leaf, Eur. J. Biochem. 181 (1989) 443–451.

[38] U.K. Laemmli, Cleavage of structural proteins during the assembly of the head of bacteriophage T4, Nature 227 (1970) 680–685.

[39] J. Rivoal, S. Trzos, D.A. Gage, W.C. Plaxton, D.H. Turpin, Two unrelated phospho*enol*pyruvate carboxylase polypeptides physically interact in the high molecular mass isoforms of this enzyme in the unicellular green alga *Selenastrum minutum*, J. Biol. Chem. 276 (2001) 12588–12597.

[40] K.J. Ellis, J.F. Morrison, Buffers of constant ionic strength for studying pH-dependent processes, Methods Enzymol. 87 (1982) 405–426.

[41] O. Emanuelsson, H. Nielsen, S. Brunak, G. von Heijne, Predicting subcellular localization of proteins based on their N-terminal amino acid sequence, J. Mol. Biol. 300 (2000) 1005–1016.

[42] M. Boden, J. Hawkins, Prediction of subcellular localization using sequence-biased recurrent networks, Bioinformatics 21 (2005) 2279–2286.

[43] K. Nakai, M. Kanehisa, Expert system for predicting protein localization sites in gram-negative bacteria, Proteins 11 (1991) 95–110.

[44] J.D. Bendtsen, H. Nielsen, G. von Heijne, S. Brunak, Improved prediction of signal peptides: SignalP 3.0, J. Mol. Biol. 340 (2004) 783–795.

[45] H. Nielsen, J. Engelbrecht, S. Brunak, G. von Heijne, Identification of prokaryotic and eukaryotic signal peptides and prediction of their cleavage sites, Protein Eng. 10 (1997) 1–6.

[46] F. Baneyx, Recombinant protein expression in *Escherichia coli*, Curr. Opin. Biotechnol. 10 (1999) 411–421.

[47] M. Higy, T. Junne, M. Spiess, Topogenesis of membrane proteins at the endoplasmic reticulum, Biochemistry 43 (2004) 12716–12722.
[48] J.F. Turner, L. Copeland, Hexokinase II of pea seeds, Plant Physiol. 68 (1981) 1123–1127.
[49] L. Copeland, M. Morell, Hexose kinases from the plant cytosolic fraction of soybean nodules, Plant Physiol. 79 (1985) 114–117.
[50] D.C. Doehlert, Separation and characterization of four hexose kinases from developing maize kernels, Plant Physiol. 89 (1989) 1042–1048.
[51] E.M. Farré, A. Tiessen, U. Roessner, P. Geigenberger, R.N. Trethewey, L. Willmitzer, Analysis of the compartmentation of glycolytic intermediates, nucleotides, sugars, organic acids, amino acids, and sugar alcohols in potato tubers using a nonaqueous fractionation method, Plant Physiol. 127 (2001) 685–700.
[52] J.T. van Dongen, G.W. Roeb, M. Dautzenberg, A. Froehlich, H. Vigeolas, P.E. Minchin, P. Geigenberger, Phloem import and storage metabolism are highly coordinated by the low oxygen concentrations within developing wheat seeds, Plant Physiol. 135 (2004) 1809–1821.
[53] S. Cortès, M. Gromova, A. Evrard, C. Roby, A. Heyraud, D.B. Rolin, P. Raymond, R.M. Brouquisse, In plants, 3-*O*-methylglucose is phosphorylated by hexokinase but not perceived as a sugar, Plant Physiol. 131 (2003) 824–837.
[54] M. Paul, T. Pellny, O. Goddijn, Enhancing photosynthesis with sugar signals, Trends Plant Sci. 6 (2001) 197–200.
[55] H. Schluepmann, T. Pellny, A. van Dijken, S. Smeekens, M. Paul, Trehalose 6-phosphate is indispensable for carbohydrate utilization and growth in *Arabidopsis thaliana*, Proc. Natl. Acad. Sci. USA 100 (2003) 6849–6854.
[56] J.M. Thevelein, S. Hohmann, Trehalose synthase: guard to the gate of glycolysis in yeast? Trends Biochem. Sci. 20 (1995) 3–10.
[57] P.J. Eastmond, A.J. van Dijken, M. Spielman, A. Kerr, A.F. Tissier, H.G. Dickinson, J.D. Jones, S.C. Smeekens, I.A. Graham, Trehalose-6-phosphate synthase 1, which catalyses the first step in trehalose synthesis, is essential for *Arabidopsis* embryo maturation, Plant J. 29 (2002) 225–235.
[58] S. Gonzali, A. Alpi, F. Blando, L. De Bellis, *Arabidopsis* (HXK1 and HXK2) and yeast (HXK2) hexokinases overexpressed in transgenic lines are characterized by different catalytic properties, Plant Sci. 163 (2002) 943–954.
[59] J. Salas, M. Salas, E. Viñuela, A. Sols, Glucokinase of rabbit liver, purification, and properties, J. Biol. Chem. 240 (1965) 1014–1018.
[60] L. Guglielminetti, P. Perata, A. Morita, E. Loreti, J. Yamaguchi, A. Alpi, Characterization of isoforms of hexose kinases in rice embryo, Phytochemistry 53 (2000) 195–200.
[61] R. Gerhardt, M. Stitt, H. Heldt, Subcellular metabolite levels in spinach leaves. Regulation of sucrose synthesis during diurnal alterations in photosynthetic partitioning, Plant Physiol. 83 (1987) 399–407.
[62] S. Lalonde, D. Wipf, W.B. Frommer, Transport mechanisms for organic forms of carbon and nitrogen between source and sink, Annu. Rev. Plant Biol. 55 (2004) 341–372.
[63] M.A. Hooks, G.C. Shearer, J. Roberts, Nucleotide availability in maize (*Zea mays* L.) root tips (estimation of free and protein-bound nucleotides using 31P-nuclear magnetic resonance and a novel protein–ligand-binding assay), Plant Physiol. 104 (1994) 581–589.
[64] J.K. Roberts, J. Callis, D. Wemmer, V. Walbot, O. Jardetzky, Mechanisms of cytoplasmic pH regulation in hypoxic maize root tips and its role in survival under hypoxia, Proc. Natl. Acad. Sci. USA 81 (1984) 3379–3383.
[65] J.M. Bouny, P.H. Saglio, Glycolytic flux and hexokinase activities in anoxic maize root tips acclimated by hypoxic pretreatment, Plant Physiol. 111 (1996) 187–194.